nature COMMUNICATIONS

ARTICLE

Received 23 Dec 2011 | Accepted 24 Feb 2012 | Published 27 Mar 2012

DOI:10.1038/ncomms1759

Poly(ADP-ribose) controls DE-cadherin-dependent stem cell maintenance and oocyte localization

Yingbiao Ji[1] & Alexei V. Tulin[1]

Within the short span of the cell cycle, poly(ADP-ribose) (pADPr) can be rapidly produced by poly(ADP-ribose) polymerases and degraded by poly(ADP-ribose) glycohydrolases. Here we show that changes in association between pADPr and heterogeneous nuclear ribonucleoproteins (hnRNPs) regulate germline stem cell (GSC) maintenance and egg chamber polarity during oogenesis in *Drosophila*. The association of pADPr and Hrp38, an orthologue of human hnRNPA1, disrupts the interaction of Hrp38 with the 5′-untranslated region of DE-cadherin messenger RNA, thereby diminishing DE-cadherin translation in progenitor cells. Following the reduction of DE-cadherin level, GSCs leave the stem cell niche and differentiate. Defects in either pADPr catabolism or Hrp38 function cause a decrease in DE-cadherin translation, leading to a loss of GSCs and mislocalization of oocytes in the ovary. Taken together, our findings suggest that Hrp38 and its association with pADPr control GSC self-renewal and oocyte localization by regulating DE-cadherin translation.

[1] Cancer Biology Program, Epigenetics and Progenitor Cell Program, Fox Chase Cancer Center, Philadephia 19111, USA. Correspondence and requests for materials should be addressed to A.V.T. (Alexei.Tulin@fccc.edu).

In *Drosophila*, oogenesis begins with the asymmetrical division of one germline stem cell (GSC) into two: one GSC for self-renewal and one cystoblast that differentiates within the germarium[1]. Maintenance of GSCs is controlled by several pathways[2–6], including the regulation of DE-cadherin expression that promotes anchoring of GSC to its niche through adherens junctions (AJs)[6]. Subsequently, one GSC daughter cell, the cystoblast, loses contact with the GSC niche and divides four times to form a cyst consisting of 15 nurse cells and an oocyte[7]. On completion of proliferation, migration and differentiation of follicle stem cells in the middle of the germarium, a monolayer of follicle cells surrounds this 16-cell cyst to form an egg chamber[8]. During the last germarial stage, the elevated DE-cadherin-dependent adhesion between the oocyte and its surrounding follicle cells helps anchor the oocyte in the posterior pole, establishing the anterior–posterior axis of an egg chamber[9,10].

Heterogeneous nuclear ribonucleoproteins (HnRNPs) are ubiquitous RNA-binding proteins associated with pre-messenger RNA(mRNA)/mRNA in the nucleus and/or cytoplasm of the cell during transcription and post-transcriptional possesses[11–17]. Poly(ADP-ribose) (pADPr), a polymer formed from 2 to 200 ADP-ribose units, is produced by poly(ADP-ribose) polymerase-1 (PARP1) using NAD as a substrate[19]. Non-covalent association of PARP1–pADPr with hnRNP decorates this protein with negative charges and prevents its binding to RNA[19]. This regulation depends on the activity of PARP1, which adds pADPr to proteins[19], and poly(ADP-ribose) glycohydrolase (PARG), which removes pADPr[20].

Our present study demonstrates that pADPr association with hnRNPs controls DE-cadherin expression. We show that a high level of pADPr titrates Hrp38—an orthologue of human hnRNPA1—away from DE-cadherin mRNA and blocks Hrp38-dependent translation. Furthermore, we show that pADPr binding to Hrp38 is essential for GSC function and oocyte positioning during oogenesis.

Results

pADPr is enriched in *Drosophila* ovary. We determined the level of pADPr accumulation in different tissues of adult *Drosophila* by western blotting. The largest amount of pADPr accumulated in the ovary, for which multiple bands of pADPr were observed (Fig. 1a). To track *in vivo* pADPr accumulation in the ovary, we cultured a dissected *Drosophila* ovary in the presence of biotinylated NAD ($_b$NAD). Previously, we reported that PARP1 converts $_b$NAD into $_b$pADPr[21]. We examined 437 germaria and observed 31 dividing GSCs, all exhibiting the highest level of biotin labelling (Fig. 1b–d). GSCs in the interphase did not incorporate any $_b$NAD (Fig. 1c,d). Severe 'punctate' labelling by $_b$NAD was detected in cystoblasts (Fig. 1c,d, arrows). High levels of biotin labelling persisted during maturation of germline cysts starting from region 1 of germarium (Fig. 1c–e), yet labelling was depleted in the oocyte in stage 9 (Fig. 1f). These findings indicate the potential importance of pADPr turnover for progression of early oogenesis.

The *Parg* gene is required for oocyte localization. As PARG removes pADPr to promote dynamic turnover of pADPr, we expected to find that PARG is required for normal oogenesis. Indeed, we detected *Parg* mRNAs in follicle and germline cells in wild-type ovaries using RNA *in situ* hybridization with an antisense *Parg* RNA

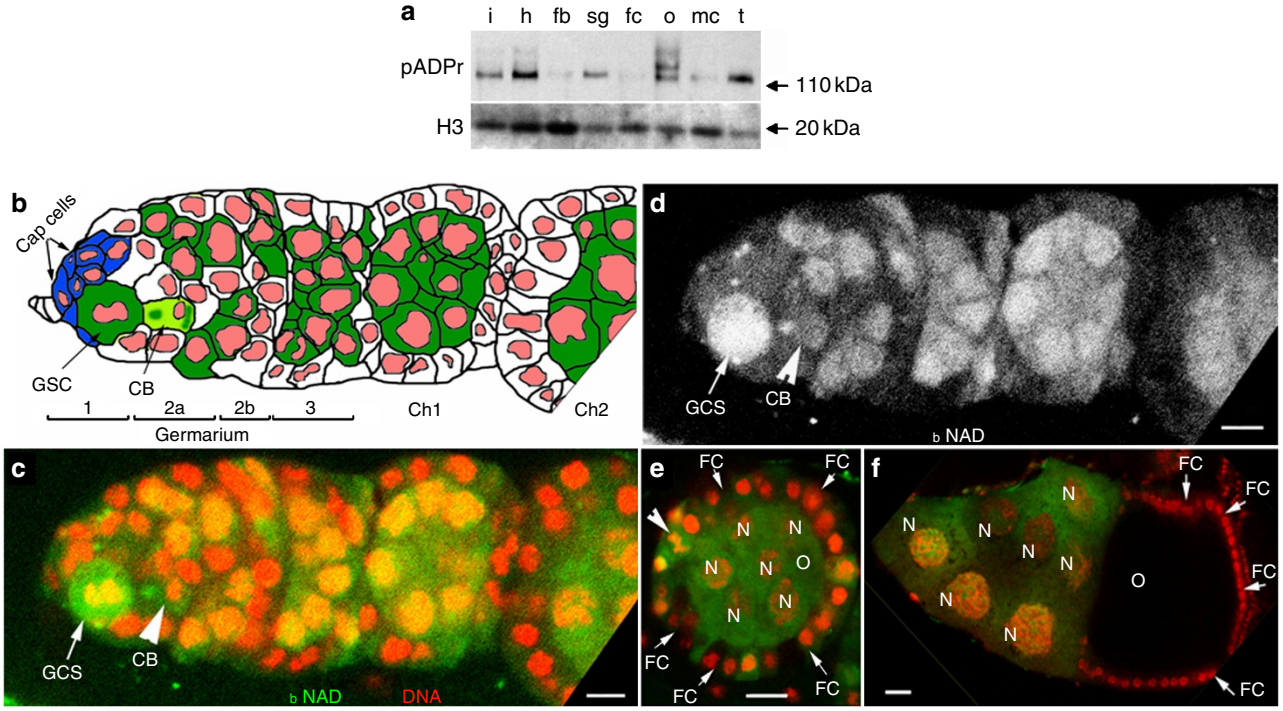

Figure 1 | pADPr accumulates in mitotic germline stem cell and cystoblast. (**a**) The comparison of total cellular pADPr level in different tissues of *Drosophila* adult by western blotting. The total protein from different tissues was immunoblotted with anti-pADPr antibody. The same blot was stripped and detected with anti-H3 antibody for loading control. fb: fat bodies; fc: female carcasses; h: heads; i: intestines; mc: male carcasses; o: ovaries; sg: salivary glands; t: testes. (**b**) Schematic illustration of anterior part of *Drosophila* ovariole (matching **c** and **d**). Cap cells (blue) form germline stem cell (GSC) niche. CB: cystoblast; Ch1,Ch2: egg chambers 1 and 2. Germline cells are shown in green. Nuclei are shown in red. (**c**–**f**) Incorporation of the biotinylated NAD ($_b$NAD) into *in vitro* cultured *Drosophila* ovary. $_b$NAD was detected using Avidin-Rhodamine staining (green). DNA was detected using oligreen dye (red). Strong accumulation of $_b$NAD within dividing germline stem cell (GSC; arrow), cystoblast (CB; arrow) and in maturating germline cysts. (**c**) Germarium and egg chamber 1. (**d**) Germarium and egg chamber 1 (only $_b$NAD is shown). (**e**,**f**) Egg chamber stages 4 (**e**) and 9 (**f**). FC: follicle cells; N: nurse cells; O: oocyte. Arrowhead indicates follicle cell in mitosis. Scale bars, 10 μm.

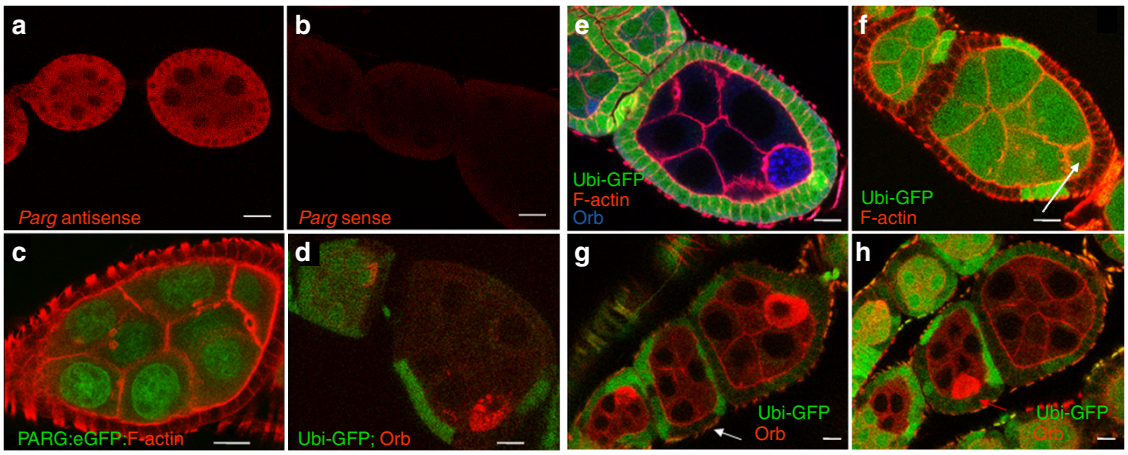

Figure 2 | *Parg* expression in the ovary and mislocalization of the oocyte caused by *Parg* mutant clones. The anterior pole of all egg chambers is to the left, and the posterior pole is to the right. (**a**) *Parg* mRNA expression in the ovary of the wild type (*y,w*) detected by RNA *in situ* hybridization using *Parg* antisense probe. (**b**) The control of RNA *in situ* hybridization using *Parg* sense probe. (**c**) The expression of PARG-EGFP in the ovary induced by germline-specific GAL4 drivers. (**d**) The mock wild-type clones, including germline and polar follicle cells, showing the normal localization of the oocyte in the posterior. The oocyte is labelled with anti-orb antibody (red). The clones are generated from the female adults (*FRT101/FRT101, ubi-GFP; FLP38/+*) after heat shock. (**e**) *Parg* mutant germline clones showing the normal localization of the oocyte in the posterior. The germline clones are generated from the female adults ($Parg^{27.1}$, *FRT101/FRT101, ubi-GFP; hs-FLP38/+*) after heat shock. *Parg* mutant germline clones are shown by the absence of GFP expression (green); F-actin is stained with phalloidin to visualize the cell membrane, and the oocyte is labelled with anti-orb antibody (blue). (**f**) *Parg* mutant follicle cell clones showing the normal localization of the oocyte in the posterior. The follicle cell clones are generated from the female adults ($Parg^{27.1}$, *FRT101/FRT101, ubi-GFP; en-Gal4,UAS-FLP38/+*). *Parg* mutant follicle cell clones are shown by the absence of GFP expression (green). F-actin is stained with phalloidin to visualize the cell membrane. Arrow indicates the oocyte shown by the enrichment of F-actin in the ring canal. (**g**) *Parg* mutant germline and follicle cell clones in the anterior (white arrow). (**h**) *Parg* mutant clones, including germline and follicle cells, showing mislocalization of the oocyte in the lateral (red arrow). (**g**,**h**) *Parg* mutant germline and follicle cell clones are generated from the female adults ($Parg^{27.1}$,*FRT101/FRT101,ubi-GFP; hs-FLP38/+*) after heat shock and shown by the absence of GFP expression (green), and the oocyte is labelled with anti-orb antibody (red). Scale bars, **a**, **b**, **g** and **h**, 10 μm; **c**-**f**, 20 μm.

probe (Fig. 2a,b, Supplementary Methods). Ectopically expressed PARG-EGFP (Enhanced GFP) was localized to the nucleoplasm of nurse cells and the oocyte in stage 7 egg chambers, confirming that PARG recycles pADPr in nuclei of the ovary cells (Fig. 2c). To test whether the *Parg* gene is essential for oogenesis, we generated *Parg* mutant clones in the ovary using the FRT/FLP system. Wild-type clones (Fig. 2d) as well as egg chambers with *Parg* mutant germline clones only ($n=73$) or follicle cell clones only ($n=91$) did not show oocyte mislocalization (Fig. 2e,f). However, egg chambers bearing *Parg* mutant clones, both in the follicle cells, including the polar cells, and the germline cells, exhibited mislocalization of the oocyte to its midpoint (36% ($n=45$), Fig. 2g,h). These results show that loss of *Parg* in both germline and polar cell clones is a precondition for oocyte mislocalization in the *Parg* mutant.

The *hrp38* mutants have reduced fertility. To characterize the functions of the *hrp38* gene during *Drosophila* development, we used one P-element insertion in exon 2 of the *hrp38* gene (w^{*},*P[XP]*^{d05172}/*TM6B, Tb*^{1})[22] and a *hrp38* region deficiency line (w^{1118}; *Df(3R)*^{Exel6209}, *P{XP-U}*^{Exel6209}/*TM6B, Tb*^{1}) having a small deletion in exon 2 of the *hrp38* gene[23] (Supplementary Fig. S1a). These mutations are lethal when homozygous. The *hrp38* hemizygotes (*hrp38*^{d05172}/*Df*) did not express *hrp38* mRNA (Supplementary Fig. S1b), and had a significantly lower expression of Hrp38 protein than the wild type at the third-instar larvae stage (Supplementary Fig. S1c). In the complementation test, the P-element insertion (*hrp38*^{d05172}) failed to complement the *hrp38* deficiency (Supplementary Table S1). Three-fourths of the *hrp38* hemizygotes (*hrp38*^{d05172}/*Df*; $n=682$) died before the pupal stage, indicating the importance of *hrp38* for normal fly development. The incomplete penetrance may have proceeded from a partial overlap of *hrp38* and *hrp36*, whose functional domains are highly homologous[24].

hrp38 RNA interference (RNAi) lines (P{GD14939}v29523 and P{GD14939}v29524/CyO) were crossed with strains ubiquitously expressing GAL4 (*Act5C–GAL4* and *tubP–GAL4*). The results show that *hrp38* RNAi causes lethality (Supplementary Table S1). The expression of a *UAS-Hrp38:RFP* transgene induced by the ubiquitously expressed arm-*GAL4* driver was sufficient to rescue lethality of the hemizygotes (*hrp38*^{d05172}/*Df*) (Supplementary Fig. S1d and Table S2). These results confirm that mutations of the *hrp38* gene are fully responsible for lethality of the hemizygotes (*hrp38*^{d05172}/*Df*). We observed that hemizygous female escapers had very low fertility (6 progeny per fly in the mutant versus 51 progeny per fly in the wild type after 5 days of crossing; $n=100$) and significantly reduced egg laying rates (0.1 egg per hour per fly versus 1.2 eggs per hour per fly, respectively), confirming that the *hrp38* gene is required for oogenesis.

The *hrp38* gene regulates oocyte localization. As the *hrp38* mutants have reduced fertility, *hrp38* functions during oogenesis were investigated. We observed that the Hrp38:GFP fusion protein in a protein trap line (ZCL588), in which GFP was spliced in the frame with the Hrp38-PE transcript[19], was predominantly expressed in the nuclei of the somatic follicle cells and germline cells during all stages of oogenesis (Fig. 3a,b). As Hrp38:GFP expression is absent in the oocyte from stage 2 (Fig. 3b), it appears that Hrp38 expression is inhibited in the oocyte once the cyst moves down the germarium after the anterior–posterior axis is established. Therefore, we compared progression of oogenesis in the wild-type and *hrp38* mutant.

In a wild-type ovariole, all oocytes showing stronger Orb staining were positioned in the posterior pole adjacent to a pair of polar follicle cells stained with FasIII (Fig. 3c). *hrp38* mutant females displayed defects during egg development, including fused egg chambers (7%, $n=125$, Fig. 3d) and mislocalization of the oocyte (11%, $n=142$,

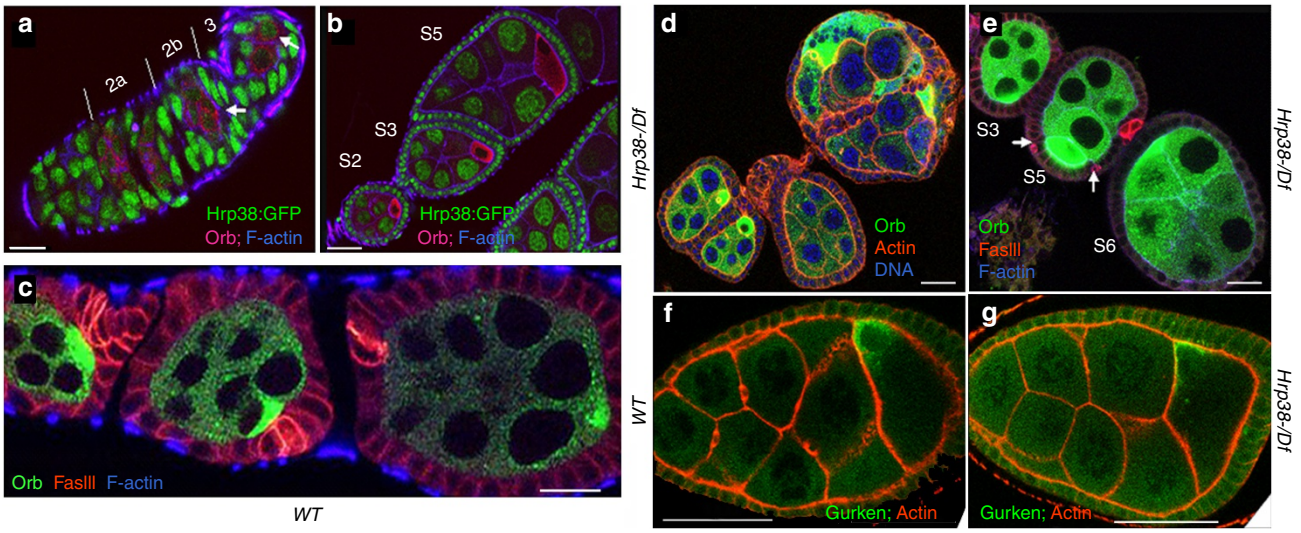

Figure 3 | Ovary developmental defects caused by the *hrp38* mutations. (**a**–**e**) Egg chambers stained with phalloidin to visualize filamentous actin in the cell membrane and anti-orb antibody to label the oocyte. The anterior pole of all the egg chambers is to the left, and the posterior pole is to the right. (**a**) The Hrp38:GFP expression pattern in the germarium. Arrows indicate the pre-oocytes in region 2b and the oocyte in region 3. (**b**) The Hrp38:GFP expression pattern in the stage 2, 3 and 5 egg chambers. (**c**) The wild type in which the oocyte is localized in the posterior pole. The egg chambers were stained with anti-FasIII (red) for labelling the polar cells. (**d**) The *hrp38* hemizygotes showing the fused egg chambers. The egg chambers stained with Drag-5 (blue) to visualize DNA. (**e**) The *hrp38* hemizygotes showing mislocalization of the oocytes. Arrows indicate the separated polar cells stained with anti-FasIII (red) in the lateral where the oocyte is localized in the stage 5 egg chamber. (**f**,**g**) Gurken protein localization in the oocytes of the wild type (**f**) and the *hrp38* mutant (**g**). Scale bars, **a**, **b**, **d** and **e**, 10 μm; **c**, 20 μm; **f**,**g**, 30 μm.

Fig. 3e). Mispositioned oocytes in the *hrp38* mutants were found either at the anterior pole (Fig. 3e, S6 egg) or on the lateral side of the egg chamber (Fig. 3e, S5 egg). In the S5 egg, a pair of polar cells was separated from each other instead of the usual connection in the poles (Fig. 3e, S5 egg), suggesting that Hrp38 is involved in defining the follicle cell patterns. The wild-type strain showed none of these defects ($n=135$; Fig. 3c). Expression of a *UASp-hrp38:RFP* transgene in the germline cells fully rescued the defective phenotypes of the *hrp38* hemizygotes ($hrp38^{d05172}/Df$; $n=216$, Supplementary Fig. S2a,b), confirming that *hrp38* loss-of-function mutation is responsible for the observed phenotypes. Although Hrp38 function is necessary for tissue polarity and oocyte positioning (Fig. 3d,e), this protein was not required for asymmetric localization of cytoplasmic markers such as Gurken (Fig. 3f,g). According to this last observation, Hrp38 controls tissue polarization by regulating extracellular interaction rather than polarization of cytoplasm within cells.

***Parg* and *Hrp38* control DE-cadherin-dependent oocyte localization**. It is well known that the posterior localization of the oocyte requires cadherin-dependent adhesion between the follicle cells surrounding the posterior pole and the oocyte[9,10]. As reported previously[9], DE-cadherin concentration in wild-type ovaries is considerably greater at the interface between the oocyte and posterior follicle cells than between nurse cells and anterior follicle cells (Fig. 4a). In *hrp38* mutant egg chambers, DE-cadherin expression was the highest at the anterior part of the egg chamber, a condition resulting in mislocalization of the oocyte to the anterior end (Fig. 4b, green arrow). The *hrp38* mutant had lower expression of DE-cadherin at the AJs of the lateral follicle cells (Fig. 4b, yellow arrow) relative to the wild type (Fig. 4a, yellow arrow). The altered expression of DE-cadherin was shown in 20% of *hrp38*−/− mutant egg chambers ($n=130$), among which 75% had relatively higher expression in the anterior than in the posterior pole, whereas 25% had no accumulation. All these egg chambers displayed either oocyte mislocalization or fused egg chambers. Immunoblotting analysis showed that DE-cadherin expression in the *hrp38* mutant ovary was approximately threefold decreased relative to the wild-type ovary (Supplementary Fig. S3a). Germline expression of the *UASp-hrp38:RFP* transgene restored the normal expression pattern of DE-cadherin in the *hrp38* mutant egg chambers ($n=90$; Supplementary Fig. S2c), confirming that *hrp38* loss-of-function causes decreased DE-cadherin expression in the ovary.

To test whether reduced expression of DE-cadherin is responsible for oocyte mislocalization in the *hrp38* mutants, we cloned the *DE-cadherin* coding region without its 5′-untranslated region (UTR) into *pUASp* vector and used nos-GAL4 to drive expression of the transgene in germline cells in the *hrp38* mutant background (Supplementary Fig. S3a). DE-cadherin expression in the germline cells was sufficient to restore normal oocyte localization in the *hrp38* mutants ($n=112$; Supplementary Fig. S3b,c). After expressing DE-cadherin transgene in the germline cells, we did not observe any phenotypes exhibited by the *hrp38* mutant ($n=136$, Supplementary Fig. S3d,e). This finding shows that proper oocyte polarity established by DE-cadherin-mediated AJs in the germarium also affects the fate of stalk and polar follicle cells in the later stages of oogenesis. Taken together, these results suggest that decreased DE-cadherin expression in the germline cells is the underlying cause for the observed phenotypes in the *hrp38* mutant.

Consistent with oocyte mislocalization observed in *Parg* mutant follicle and germline cell clones (Fig. 2g,h), the loss of *Parg* in both germ cells and polar cells led to loss of DE-cadherin expression (compare Fig. 4c with e). Expression of a *pUASp-DE-cadherin* transgene without its 5′UTR in the germline cell using nos-Gal4 driver was sufficient to rescue the oocyte mislocalization in the *Parg* mutant follicle, including the polar cells and germline cell clones ($n=34$, Fig. 4g,h). Therefore, loss of DE-cadherin expression is responsible for oocyte mislocalization in *Parg* mutant clones.

These results show that the *hrp38* and *Parg* genes regulate the expression of DE-cadherin, required for proper oocyte positioning. As Hrp38 shows greater association with pADPr in the *Parg* mutant than in the wild type[19], we proposed that pADPr binding to Hrp38 regulates DE-cadherin expression. To test this hypothesis,

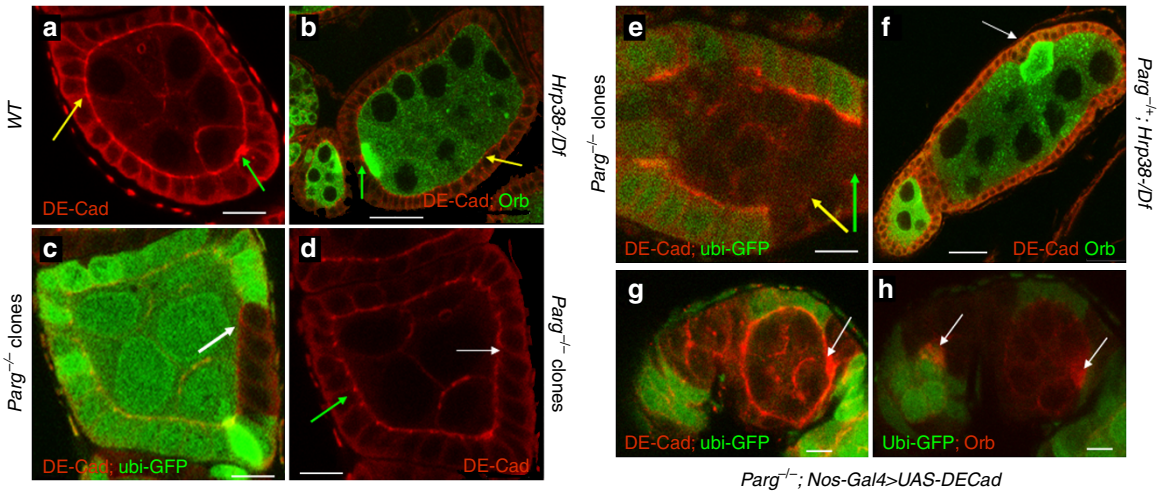

Figure 4 | Regulation of DE-cadherin expression by pADPr modification of Hrp38. The anterior pole of all the egg chambers is to the left, and the posterior pole is to the right. (**a**) DE-cadherin expression in the egg chamber of the wild type. (**b**) DE-cadherin expression in the egg chambers of the *hrp38* mutant. The oocytes were labelled with anti-orb antibody. In **a** and **b**, green arrow indicates the interface between oocyte and polar cells, and yellow arrow indicates the adherens junctions between the lateral follicle cells. (**c**) DE-cadherin expression in *Parg* follicle cell clones. *Parg* mutant follicle cell clones are shown by the absence of GFP expression. (**d**) DE-cadherin expression in the wild-type (green arrow) and *Parg* follicle cell clones (white arrow) as in **c**. Arrows in **c**,**d** indicate the adherens junctions between the lateral follicle cells. (**e**) DE-cadherin expression in *Parg* germline and follicle cell clones. *Parg* mutant germline and follicle cell clones are shown by the absence of GFP expression (green). Green arrow indicates the interface between germline cells and posterior follicle cells, and yellow arrow indicates the adherens junctions between the lateral follicle cells. (**f**) DE-cadherin expression in the egg chambers of the genotype (*Parg*−/+; $hrp38^{d05172}$/*Df*). The oocyte (white arrow) is labelled with anti-orb antibody. (**g**,**h**) Expression of DE-cadherin in the germline rescued oocyte mislocalization in *Parg* mutant clones. The full genotype is: $Parg^{27.1}$, *FRT101/Ubi-GFP, FRT101; FLP38/Nos-Gal4; UASp-DEcadherin/+*. (**g**) The elevated DE-cadherin expression (white arrow) in the posterior pole of one egg chamber with the *Parg* mutant germline and follicle cell clones, including the polar cells. (**h**) The normal oocyte localization (white arrow) in the same egg chamber as in **g**. The oocyte is labelled with anti-orb antibody (red). Scale bars, **a**–**f**, 10 μm; **g**,**h**, 5 μm.

we removed one copy of the *Parg* gene in the *hrp38* mutant background (*Parg*−/+; hrp^{d05172}/*Df*). The mutant genotype (*Parg*−/+; hrp^{d05172}/*Df*) had an increased proportion of mislocalized oocytes relative to the *hrp38* mutant alone (19% versus 11%, respectively, $n=176$; *t*-test $P<0.05$). Most of the mislocalized oocytes in the genotype (*Parg*−/+; hrp^{d05172}/*Df*) showed no accumulation of DE-cadherin in either pole, resulting in laterally positioned oocytes (Fig. 4f, arrow), which resembled the phenotypes caused by DE-cadherin null mutation[10]. Expression of *Hrp38:RFP* ($n=152$) or *DE-cadherin* transgene ($n=165$) in the germline fully rescued oocyte mislocalization in (*Parg*−/+; hrp^{d05172}/*Df*).

***Hrp38* controls GSC maintenance**. Besides oocyte localization, DE-cadherin is required for GSC maintenance by anchoring GSCs within the niche through AJs[6] (Fig. 5a). If controlling DE-cadherin levels is a general function of pADPr binding to Hrp38, *hrp38* and *Parg* mutants should display defects in DE-cadherin-mediated regulation of GSCs. Indeed, we found that Hrp38:GFP is expressed in GSCs, as well as in cap cells of the GSC niche (Fig. 5b). Similar to the wild type (n = 85), most germaria of *hrp38* mutants had two or three GSCs at day 3 after eclosion ($n=82$) (Supplementary Fig. S4a). At day 10, wild-type germaria had two or three GSCs ($n=94$; Fig. 5c), although most germaria in the *hrp38* mutant (72%) had only one GSC left ($n=91$; Fig. 5d and Supplementary Fig. S4a). At 17 days after eclosion, 70% of germaria in the *hrp38* mutants had lost their GSCs ($n=96$; Fig. 5e,f and Supplementary Fig. S4a), whereas the wild type still retained GSC self-renewal ability ($n=90$; Fig. 5f). The expression of the *hrp38:RFP* transgene in the germline cells restored GSC self-renewal ability of the *hrp38* mutant (Fig. 5f, Supplementary Fig. S4a,b), confirming that the *hrp38* gene is required for GSC maintenance.

DE-cadherin is strongly expressed in the interface between GSCs and cap cells in the wild-type fly[6] for anchoring the GSC within the niche (Fig. 5g). We examined DE-cadherin expression in 10-day-old wild-type and *hrp38* mutant GSCs (Fig. 5g,h). DE-cadherin expression level at the interface between the cap cells and the one remaining GSC in 10-day-old *hrp38* mutants was reduced by 70%, relative to that in the wild type ($n=10$, Fig. 5h). Normal expression levels of DE-cadherin in the interface between cap cells and GSC were restored by expressing *UASp-hrp38:RFP* transgene in GSCs in 14-day-old *hrp38* mutants ($n=128$, Supplementary Fig. S4c). Ectopic expression of DE-cadherin in the germline significantly increased the GSC self-renewal ability in the *hrp38* mutant background (Figs 5f, Supplementary Fig. S4d–f), confirming that decreased DE-cadherin expression causes the loss of GSC self-renewal ability in the *hrp38* mutants.

To maintain their undifferentiated state, GSCs must maintain low levels of the Bag-of-marbles (BAM) differentiation factor[25–27]. Compared with the wild-type fly ($n=54$, Supplementary Fig. S5a), BAM was not prematurely expressed in the *hrp38* mutant GSCs ($n=58$, Supplementary Fig. S5b). Using anti-cleaved Caspase-3 antibody, which has been used successfully to detect apoptosis in the *Drosophila Lsd1* mutant GSC[28], no strong apoptosis signals were detected in the GSC of 10-day-old *hrp38* mutants ($n=58$, Supplementary Fig. S5b). These observations largely exclude the possibility that either premature differentiation of GSC through the BAM-dependent pathway or apoptosis caused the loss of GSC maintenance in the *hrp38* mutant.

***Parg* controls DE-cadherin-dependent stem cell maintenance**. Because *Parg* mutant germline cell and follicle cell clones lost the expression of DE-cadherin (Fig. 4e), we investigated whether *Parg* is required for GSC self-renewal. We found that *Parg* mRNA and PARG-EGFP are expressed in the wild-type GSCs (Fig. 6a and Supplementary Fig. S5c) and by germline-specific GAL4 driver (Fig. 6b). To determine whether *Parg* is required for GSC self-renewal, we used a

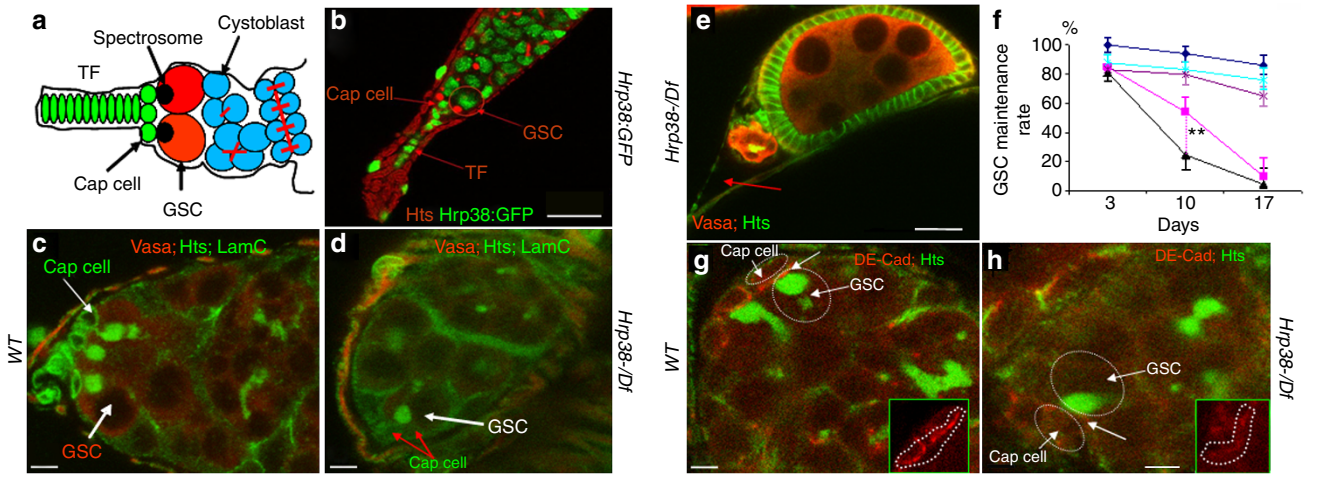

Figure 5 | The *hrp38* gene is required for maintenance of germline stem cells. (**a**) Simplified diagram of the germarium structure. GSCs having the round spectrosome are localized in the niche containing terminal filament (TF) and cap cells. The cystoblast and its progeny are interconnected through the ring canals. (**b**) The *hrp38* expression in GSC and cap cells in the tip of germarium of the Hrp38:GFP strain. GSC is labelled with anti-hts antibody for spectrosome (red). (**c**) Ten-day-old germarial tip of the wild type. (**d**) Ten-day-old germarial tip of the *hrp38* mutant. In **c** and **d**, GSCs are labelled with anti-hts (green) and anti-Vasa antibody (red). The cap cells are labelled with anti-Lam-C antibody (green). (**e**) Seventeen-day-old germarium of the *hrp38* mutant showing the last egg chamber. The fusome in the last egg chamber is shown as yellow after labelling with anti-hts (green) and anti-Vasa antibody (red). Arrow indicates an empty germarium. (**f**) Graph showing GSC maintenance rate of the indicated genotypes. The GSC maintenance rate was based on the percent of the germaria with two to three GSCs at the indicated time after eclosion. Two germaria with one GSC was counted as one wild-type germarium to calculate their maintenance rate. Symbols: dark blue line with diamonds (the wild type; $n=85$); pink line with squares (*hrp38−/−*; $n=82$); black line with triangles (*Parg+/−*; *hrp38−/−*; $n=80$); light blue with crosses (*RFP:Hrp38/nos-Gal4*; *hrp38−/−*; $n=92$); dark magenta line with stars (*DE-cad/nos-Gal4*; hrp38−/−; $n=110$). The error bar represents the standard deviation of the proportion normalized with the sample size. $^{**}P<0.01$, analysed by *t*-test. (**g**) DE-cadherin expression in the 10-day-old GSC in the wild type. (**h**) DE-cadherin expression in the 10-day-old GSCs in the *hrp38* mutant. In **g** and **h**, GSCs are labelled with anti-hts (green). Insets showed DE-cadherin expression in the interface (arrows) between GSC and the cap cells (circled). Scale bars, **b**, **e**, 10 μm; **c**, **d**, **g**, **h**, 5 μm.

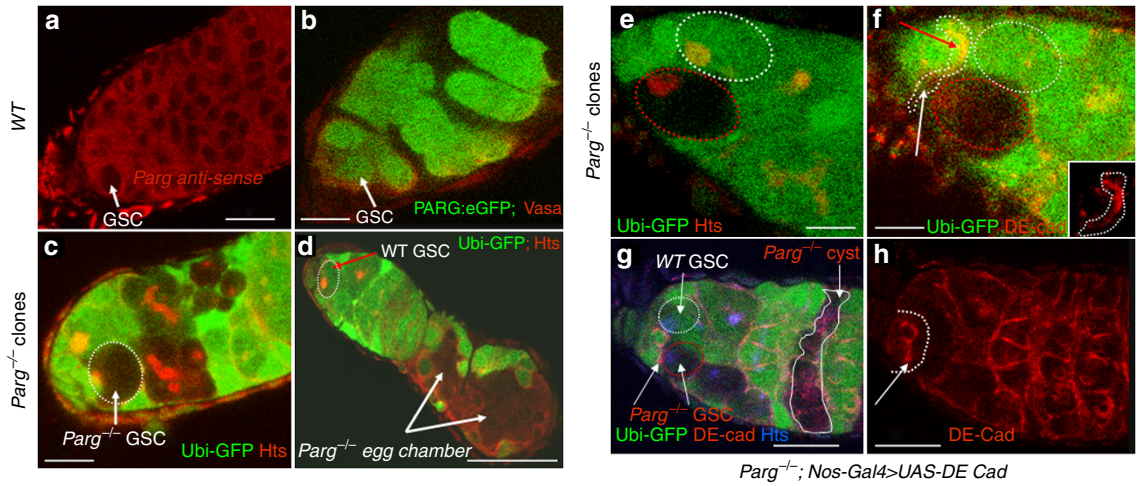

Figure 6 | Loss of DE-cadherin expression in *Parg* mutant GSC. (**a**) *Parg* mRNA expression in GSC in the wild type (y,w), as detected by RNA *in situ* hybridization using *Parg* antisense probe. (**b**) The expression of PARG-EGFP in GSCs by germline-specific GAL4 drivers. (**c**) Germaria showing a 3-day-old *Parg* mutant GSC with loss of GFP expression. GSC is labelled with anti-hts (red). (**d**) 17-day-old germarium showing the loss of *Parg* mutant GSC. The loss of *Parg* mutant GSC was shown by the presence of two mutant egg chambers. GSC labelled with anti-hts antibody (red). (**e**,**f**) DE-cadherin expression in a germarium tip carrying one wild-type GSC and one *Parg* mutant GSC 1 week after clone induction. White circle: the wild-type GSC (GFP positive); Red cycle: *Parg* mutant GSC (GFP-negative); GSCs are labelled with anti-hts antibody in **e**. Inset in **f** shows DE-cadherin expression in the interface between GSCs and wild-type cap cells (arrow indicated in **f**). (**g**) 17-day-old germarium showing *Parg* mutant GSC and its progeny. (**h**) Expression of DE-cadherin in the germline cells rescued *Parg* mutant GSC loss as shown in **g**. The full genotype (**g** and **h**): *Parg* $^{27.1}$, *FRT101/Ubi-GFP, FRT101; FLP38/Nos-Gal4; UASp-DEcadherin/+*. GSC labelled with anti-hts antibody (blue). Arrows in **g** and **h** indicate DE-cadherin expression in the interface between GSCs and wild-type cap cells. Scale bars, **a**–**c**, **e**–**h**, 10 μm; **d**, 20 μm.

FLP/FRT recombination system to generate negatively labelled *Parg* mutant GSCs, which were identified by the absence of GFP expression (Fig. 6c,d). The loss rates of the mutant GSCs were computed based on a published procedure[6]. Three days after clone induction, *Parg* mutant GSCs and cysts were present in the germarium ($n=53$; Fig. 6c). Two weeks after clone induction, *Parg* mutant GSCs

were lost in 95% of the germaria ($n=58$, Supplementary Fig. S5d) where the developing *Parg* mutant egg chamber was visible (Fig. 6d). Marked wild-type GSCs were still retained in 80% of germaria ($n=56$, Supplementary Fig. S5d). Therefore, we conclude that *Parg* is required for maintaining GSCs and infer that poly(ADP-ribosyl)ation strongly affects GSC maintenance.

To test whether the *hrp38* and *Parg* genes interact to control GSC maintenance, we assessed the changes in number of GSCs in (*Parg*−/+;*hrp*^{d05172}/*Df*) genotype with aging. Removing one copy of the *Parg* gene caused a more rapid GSC loss in the *hrp38* mutant (Fig. 5f and Supplementary Fig. S4a). Expression of *Hrp38:RFP* or *DE-cadherin* transgenes in the germline fully restored GSC maintenance ability (*Parg*−/+;*hrp*^{d05172}/*Df*; Supplementary Fig. S4a). These results demonstrate that genetic interaction between the *hrp38* and *Parg* genes controls GSC maintenance.

Further, we examined DE-cadherin expression in *Parg* mutant GSC clones 1 week after clone induction. DE-cadherin accumulated in the interface between the wild-type GSC (GFP-positive) and wild-type cap cells, yet its expression was fourfold reduced in *Parg* mutant GSC clones (GFP-negative) when compared with DE-cadherin accumulation in wild-type GSC cells (Fig. 6e,f; $n=10$). With expression of the *DE-cadherin* transgene in the germline cells (Fig. 6g,h), the *Parg* mutant GSCs were still maintained in 65% of germaria ($n=70$) 2 weeks after clone induction, which is comparable to the maintenance rate of the marked wild-type GSCs (Supplementary Fig. S5d). Therefore, the loss of DE-cadherin expression, resulting in the failure to strongly anchor the *Parg* mutant GSC within the niche by AJs, likely explains the *Parg* mutant's loss of GSC self-renewal. Similar to *hrp38* mutant GSCs, *Parg* mutant GSCs were lost neither by apoptosis (Supplementary Fig. S5e,f) nor by inappropriate expression of Bam (Supplementary Fig. S5g,h).

pADPr inhibits Hrp38-dependent DE-cadherin translation. To further evaluate how pADPr binding to Hrp38 controls DE-cadherin expression, we examined mRNA and protein expression levels of DE-cadherin in the *hrp38* and *Parg* mutants at the third-instar larval stage. No significant difference in mRNA expression levels was found between the wild-type and the *hrp38* mutant or the *Parg* mutant by quantitative reverse transcription-PCR (Supplementary Methods; Fig. 7a), suggesting that pADPr binding to Hrp38 does not affect DE-cadherin transcription. Although the *DE-cadherin* gene has only one transcript with a constitutively spliced intron (Flybase), we examined potential effects of *hrp38* or *Parg* mutation on splicing of *DE-cadherin* transcript. Splicing defects were not observed in *hrp38* and *Parg* mutants, suggesting that Hrp38 and its association with pADPr do not regulate DE-cadherin by affecting splicing. Immunoblotting analysis (Supplementary Methods) showed that protein expression levels of DE-cadherin in *hrp38* and *Parg* mutants was decreased by 3.5- and 4.0-fold, respectively, relative to the wild-type (Fig. 7b), suggesting

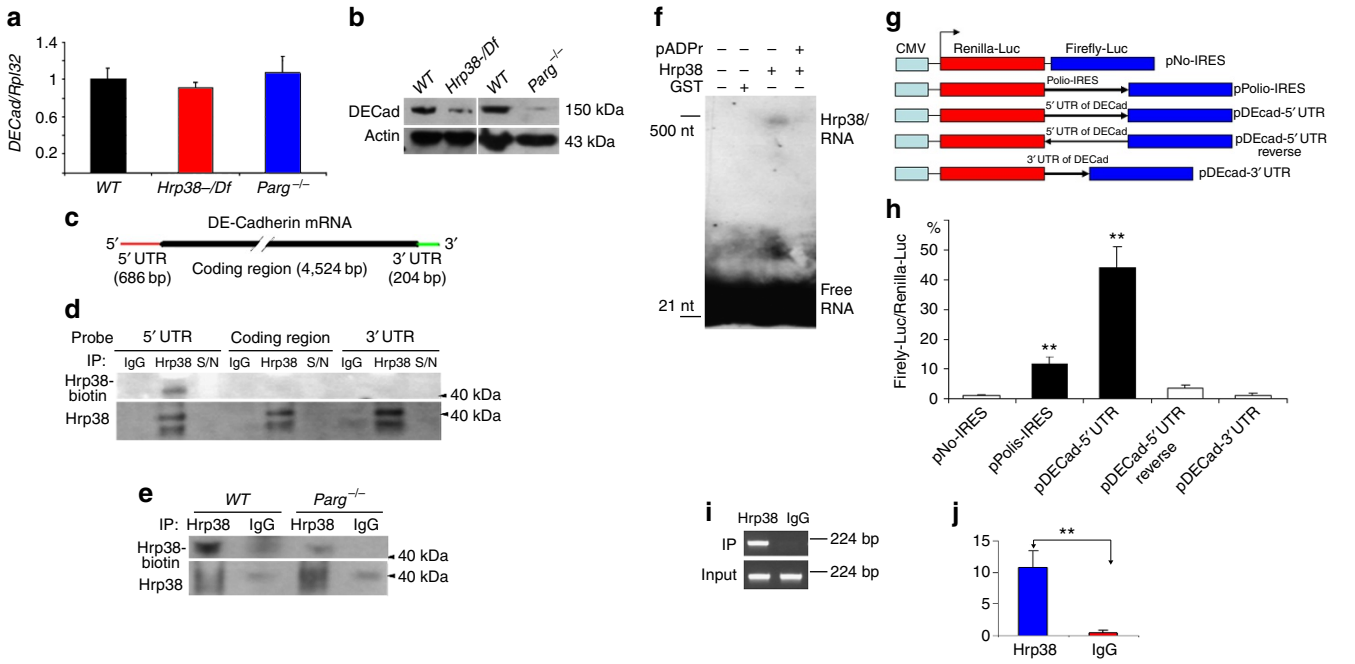

Figure 7 | pADPr disrupts Hrp38 binding to 5′UTR of DE-cadherin conferring IRES activity. (**a**) The mRNA expression level of DE-cadherin in the different genotypes at the wandering third-instar larvae stage. (**b**) The protein expression level of DE-cadherin in the different genotypes at the wandering third-instar larvae stage. (**c**) The structure of DE-cadherin transcript. The biotin-labelled probes were made from three regions (5′UTR, coding region and 3′UTR). (**d**) Hrp38 binding to 5′UTR of DE-cadherin in the ovary is shown by ultraviolet crosslinking analysis. The ovarian lysate from the wild-type fly (*y,w*) crosslinked to the biotin-labelled RNA probes as indicated was IPed with rabbit anti-Hrp38 antibody or normal rabbit IgG as the control for IP. The supernatant (S/N), which was obtained after each IP, was run in the same blot to show the efficiency of RNase treatment. (**e**) Decreased amounts of Hrp38 protein binding to 5′UTR of DE-cadherin in the *Parg* mutant. In **d** and **e**, Hrp38 protein binding to biotin-labelled RNA probe was detected with Streptavidin. The same blot was stripped and probed with anti-Hrp38 antibody to show IP efficiency. (**f**) Inhibition of Hrp38 binding to its target RNA motif by poly(ADP-ribose). The biotin-labelled G-rich RNA element (5′-CAGGGCGCGCACUGUACGAG-3′) within 5′UTR of DE-cadherin was incubated with the components as indicated. (**g**) Diagrams of the different constructs for dual luciferase assay. CMV: cytomegalovirus (CMV) promoter; pNO-IRES (negtative control); pPolio-IRES (positive control); pDEcad 5′UTR: *DE-cadherin* 5′UTR cloned into the vector in the forward orientation. pDEcad 5′UTR-reverse (spacer control); pDEcad-3′UTR (element control). (**h**) The ratio of firefly-to-Renilla luciferase activity after the transfection of the different constructs as indicated into *Drosophila* S2 cells. (**i**,**j**) The association of Hrp38 with the transcript from pDEcad 5′UTR-luciferase construct shown by regular reverse transcription (RT)-PCR (**i**) and quantitative RT-PCR (**j**) after RNA-IP. RNA-IP was done using anti-Hrp38 antibody or rabbit IgG as a control after the transfection of pDEcad-5′UTR construct into S2 cells. The error bars in **a**, **h** and **j** represents the standard deviation from three independent experiments. $^{**}P<0.01$, analysed by *t*-test.

that the association of Hrp38 with pADPr regulates DE-cadherin expression at the translational level.

Next, we tested whether Hrp38 protein could bind to DE-cadherin mRNA directly in the ovary. Using ultraviolet crosslinking, biotin-labelled probes were made from three distinct regions (5′UTR, coding region and 3′UTR) of DE-cadherin (Fig. 7c). Ultraviolet crosslinking experiments showed that Hrp38 binds only to the 5′UTR of DE-cadherin mRNA in wild-type ovaries (Fig. 7d). Association of Hrp38 with *DE-cadherin* transcripts was further verified by *in vivo* RNA immunoprecipitation (IP; Supplementary Methods) using anti-Hrp38 antibody in the *Drosophila* ovary (Supplementary Fig. S6a,b).

Our previous study demonstrated that pADPr binding to Hrp38 reduced ability of this protein to bind RNA[19]. In humans, pADPr modification is known to inhibit the RNA-binding ability of hnRNP A1[19], the mammalian homologue of Hrp38 (ref. 29). To assess the role of Hrp38 modification by pADPr in *Drosophila*, we tested whether poly(ADP-ribosyl)ation could inhibit Hrp38 binding to the 5′UTR of DE-cadherin using ultraviolet crosslinking. Total protein was extracted from wild-type or *Parg* mutant third-instar larvae and was crosslinked to the 5′UTR of DE-cadherin. The amount of Hrp38 protein binding to the 5′UTR of DE-cadherin was 3.8-fold decreased in the *Parg* mutant, relative to that in the wild-type, suggesting that association with pADPr inhibits Hrp38 binding to the 5′UTR of DE-cadherin (Fig. 7e).

Based on the finding that human hnRNPA1 has the strongest binding affinity to the G-rich RNA element (5′-UAUGAUAGG GACUUAGGGUG-3′)[30], a potential binding site of Hrp38 (413-5′-CAGGGCGCGCACUGUACGAG-3′-432 bp) was identified within the DE-cadherin 5′UTR region. To test whether Hrp38 could bind to this G-rich motif, Hrp38 proteins were generated and purified (Supplementary Fig. S6c). The dot-blot assay confirmed that pADPr binds to Hrp38 protein *in vitro* (Supplementary Fig. S6d). An electrophoretic mobility shift assay showed that Hrp38 binds to this RNA motif (Fig. 7f, lane 3). Pre-incubation of Hrp38 protein with pADPr almost completely abolished Hrp38 binding to this RNA motif (Fig. 7f, lane 4). This result confirms that pADPr strongly inhibits the interaction between Hrp38 and RNA *in vitro* and provides additional evidence that association with pADPr inhibits Hrp38 binding to the 5′UTR of DE-cadherin.

Hrp38 is required for IRES-dependent *DE-cadherin* translation. The 5′UTR (686 bp) of *DE-cadherin* is much longer than the average size of 256 bp in 5′UTR of *Drosophila* genes[31], implying that the *DE-cadherin* 5′UTR may have the ability to initiate an internal ribosome entry site (IRES)-mediated translation. Nucleotide sequence of IRES allows translation initiation in the middle of an mRNA sequence[32]. To test whether Hrp38 binding to the DE-cadherin 5′UTR promotes IRES-dependent translation, the 5′UTR of *DE-cadherin* was cloned into the upstream sequence of the firefly luciferase gene in Renilla/Firefly luciferase reporter plasmid (Fig. 7g). After transfection into *Drosophila* S2 cells, firefly and Renilla luciferase activities were measured. As a positive control, the Poliovirus IRES showed tenfold increase of luciferase activity relative to the control construct (pNo-IRES; Fig. 7h). In contrast, the luciferase activity in cells transfected with DE-cadherin 5′UTR construct (p5′UTR DE-cad) was increased 40-fold, relative to the control construct (Fig. 7h). The efficient induction of IRES-mediated translation by the DE-cadherin 5′UTR is similar to that found in the 5′UTRs of other genes in *Drosophila*[33]. Neither the DE-cadherin 5′UTR in reverse orientation, as a spacer control, nor DE-cadherin 3′UTR, as an element control, show a significant increase in firefly luciferase activity, relative to the control (Fig. 7h). Consequently, the DE-cadherin 5′UTR has a strong ability to induce IRES-mediated translation. Furthermore, *in vivo* RNA IP showed that Hrp38 was associated with the transcript from *DE-cadherin*-5′UTR luciferase construct after transfection into *Drosophila* S2 cells (Fig. 7i–j), suggesting that Hrp38 is an IRES transacting factor for promoting cap-independent translation of *DE-cadherin* mRNA.

Discussion

Our experimental findings suggest that pADPr binding to *Drosophila* hnRNPA1 homologue Hrp38 regulates stem cell maintenance and oocyte polarity (Fig. 8a–c). Earlier research demonstrated that Hrp38 regulates alternative splicing[19,34], whereas hnRNPA1 was reported to control translation initiation through an IRES-mediated mechanism by binding to the 5′UTR of regulated genes[35,36]. Here we show that pADPr association with Hrp38 controls DE-cadherin translation through an IRES-mediated mechanism. As Hrp38 binds to the 5′UTR of DE-cadherin and is associated with the *DE-cadherin* 5′UTR-luciferase transcript, it seems very likely that Hrp38 is an IRES transacting factor for promoting DE-cadherin translation. In mammals, post-translational modification of hnRNPA1 has been shown to regulate IRES-dependent translation. For instance, phosphorylation of hnRNPA1 can promote the binding of hnRNPA1 to IRES of *c-Myc* in myeloma cells[37]. Similarly, our results suggest that pADPr modification of hnRNPs negatively regulates IRES-mediated translation by inhibiting the binding of hnRNPs to IRES.

The inhibitory function of pADPr binding to hnRNPs likely occurs in the nucleus for two reasons. First, Hrp38 is predominantly a nuclear protein that binds to the 5′UTR of DE-cadherin presumably in the nucleus. Second, pADPr metabolism is mainly localized in the nucleus. This inference is consistent with a currently accepted model suggesting that IRES transacting factors, such as hnRNPA1, are associated with IRES-containing mRNA in the nucleus from the beginning[38]. However, as recent research has shown that pADPr can regulate microRNA-mediated translation in the cytoplasm[39], it is entirely plausible that poly(ADP-ribosy)lation also functions in the cytoplasm to inhibit IRES-mediated translation.

Our finding that pADPr modification of Hrp38 regulates DE-cadherin expression in the ovary reveals how DE-cadherin expression is regulated during oocyte localization. The localization of the oocyte in the posterior end occurs during the transition from region 2b to region 3 in the germarium[10]. We found that Hrp38 is also expressed in the oocyte and its surrounding follicle cells in region 2b of the germarium (Fig. 3a). We also found that the *hrp38* mutant has a lower expression of *DE-cadherin* at the interface between the oocyte and surrounding posterior cells, implying that the *hrp38* gene is required for upregulating DE-cadherin expression for oocyte localization. Therefore, we suggest that Hrp38 is required for upregulation of DE-cadherin expression in both the oocyte and surrounding follicle cells by promoting translation (Fig. 8c). The expression of Hrp38 in the oocyte and surrounding follicle cells in region 2b helps increase the translation of DE-cadherin by binding to the 5′UTR of *DE-cadherin* mRNA. The newly produced DE-cadherin assists with anchoring the oocyte in the posterior pole. In mid-body follicle cells and nurse cells, the Hrp38 association with pADPr can downregulate DE-cadherin expression (Fig. 4e). As expression of the DE-cadherin transgene in the germline was sufficient to rescue oocyte mislocalization in the *Parg* mutant double clones (Fig. 4h), our finding supports the notion that *DE-Cadherin* germline mutant clones alone are not sufficient to cause oocyte mislocalization[40,41]. In summary, we have identified a pathway that regulates stem cell maintenance and oocyte polarity via pADPr modification of an hnRNP protein (Hrp38) in *Drosophila* (see Supplementary Discussion for broader implications of these findings).

Methods

***Drosophila* strains and genetics.** Flies were cultured on standard cornmeal–molasses–agar media at 25 °C, unless otherwise indicated. The following stocks were from Bloomington Stock Centre: *arm:GAL4/Cyo* (#1560); *Act5C–GAL4/Cyo* (#4414); *tubP–GAL4/TM3* (#5538); *P{PTT-GC}Hrb98DE*^{ZCL0588} (Hrp38:GFP trap

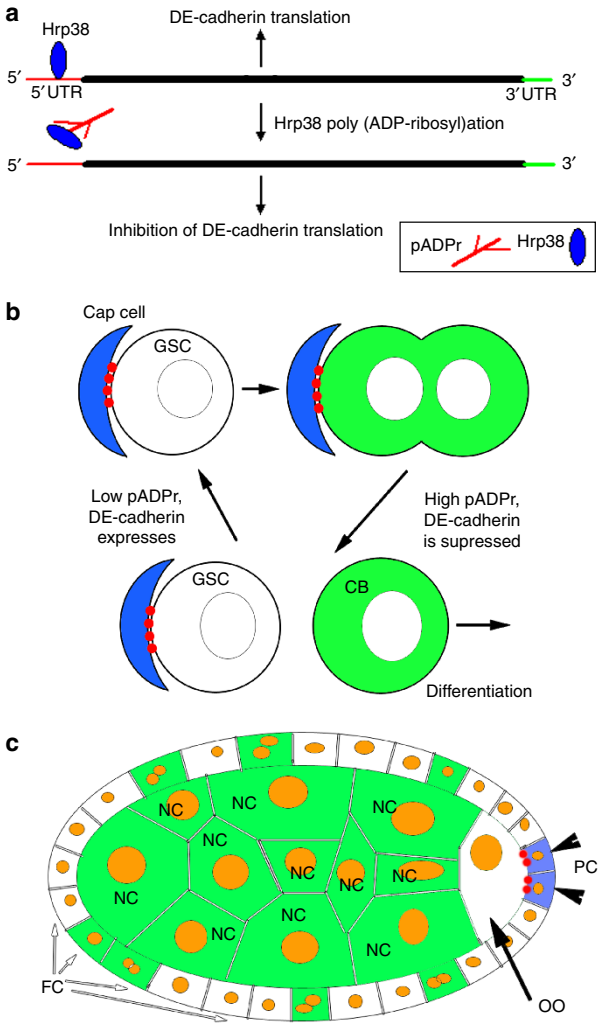

Figure 8 | Hrp38 modification by pADPr controls maintenance of GSC and oocyte localization. (**a**) pADPr binding to Hrp38 regulates DE-cadherin translation. Hrp38 binds to 5′UTR of DE-cadherin to promote translation by IRES-mediated manner. Once Hrp38 is modified with pADPr and dissociated from 5′UTR of DE-cadherin, its translation is inhibited. (**b**) pADPr modification of Hrp38 regulates DE-cadherin translation for germline stem cell (GSC) maintenance. DE-cadherin (red) accumulates in the interface between cap cells and GSC, keeping GSC in the stem cell niche. High level of pADPr (green) during mitosis and in cystoblasts suppresses translation of DE-cadherin. Suppression of DE-cadherin production promotes cystoblasts to leave stem cell niche and differentiate. (**c**) pADPr binding to Hrp38 regulates DE-cadherin translation for oocyte (OO) localization in maturating egg chamber. Low level of pADPr in the oocyte and mitotically quiescent polar cells (PC) allows translating DE-cadherin (red) and positioning the oocyte in the posterior pole of the egg chamber. High level of pADPr (green) in nurse cells and mid-body follicle cells inhibits translation of DE-cadherin. FC, follicle cells.

line, #6822); y^1, w^*, v^{24}, *P{FRT(whs^{hs})101* (#1844). A P-element insertion of the *hrp38* gene (*w*,P[XP]^{d05172}/TM6B, Tb^1*) and a *hrp38* region deficiency line (*w^{1118}; Df(3R)Exel6209, P{XP-U}Exel6209/TM6B, Tb^1*) from the Exelixis Collection at the Harvard Medical School were replaced with the GFP-bearing balancer (*TM3, P{ActGFP}JMR2, Ser^1*) for selecting homozygous mutants. Two *Hrp38* RNAi lines (*w^{1118}; P{GD14939}v29523* and *w^{1118}; P{GD14939}v29524/CyO*) were from the Vienna *Drosophila* RNAi Centre. The *Parg* mutant (*Parg $^{27.1}$/FM7, Actin-GFP*) was described previously[42]. The germline-specific GAL4 driver (*nos-Gal4*:VP16) was from Dr Spradling's lab. The BAM-GFP reporter line was a gift from Dr McKearin[27]. The full-length Hrp38 PCR fragment amplified from a *hrp38* cDNA clone (LD383464) was cloned into pUAST-RFP (carboxy-terminus fusion) and pUASp-RFP (C-terminus fusion) vectors through the *Drosophila* Gateway Vector Cloning System (Carnegie Institution of Washington). The full-length *DE-cadherin* coding region without its 5′UTR was amplified from DE-cadherin cDNA clone (RE37915; DGRC) and cloned into pUASp vector (DGRC). The pUSAp-PARG:EGFP transgene was constructed by cloning the fused fragment of PARG cDNA with EGFP into pUASp vector. All transgenic flies were obtained with the standard P-element-mediated transformation method.

Clonal analysis using the FRT-FLP system. The *Parg* female heterozygotes (*Parg$^{27.1}$/FM7a,w^a*) were crossed with *y^1*, w*, *v^{24}*, *P{FRT(whs^{hs})101/Y^{43}* to generate the FRT-bearing Parg mutation (*Parg$^{27.1}$*, *P{FRT(whs^{hs})101*/FM7a,w^a) by genetic recombination. To induce the follicle cell clones in the ovary, *Parg $^{27.1}$*, *P{FRT(whs^{hs})101*/FM7a,w^a was crossed with w*, Ubi-GFP,*P{FRT(whs^{hs})101*/Y; *P{en2.4-GAL4}e16E*, *P{UAS-FLP1.D}JD1*/Cyo[44]. To induce the Parg mutant germline clones in the ovary, the newly enclosed adults (*Parg$^{27.1}$*, *P{FRT(whs^{hs})101*/w*, Ubi-GFP,*P{FRT(whs^{hs})101*; P{hs::FLP}38/+) from the progeny of *Parg$^{27.1}$*, *P{FRT(whs^{hs})101*/FM7a crossed with *w*, Ubi-GFP,P{FRT(whs^{hs})101*/Y; *P{hsFLP}38* (a gift from Dr O'Reilly) were treated by heat-shock at 37 °C for 2 h during the daytime for 2 days. The *Parg* GSC clones were identified based on the absence of GFP expression and the presence of the round fusome labelled by anti-hts antibody. The wild-type clones were generated using the line (*y^1*, w*, *v^{24}*, *P{FRT(whs^{hs})*101) using the same method. The loss rates of the mutant GSCs were counted at 3, 10 and 17 days after clone induction, respectively, based on the published procedure[6].

Biotinylated NAD assay to detect PARP1 activity. To detect PARP1 activity *in vivo*, we used an assay based on incorporation of biotin label donated from $_b$NAD to pADPr proteins[21,45]. Biotin incorporation detected after exposure to $_b$NAD is greatly enhanced over intrinsic cytosolic biotin signal. In *Drosophila*, the utilization of NAD is, in general, PARP1-dependent[21]. To deliver $_b$NAD to tissues for the assay, we dissected *Drosophila* ovary, leaving exposed tissues in the presence of 2.5 nM $_b$NAD for 1 h. Our previous experiments[21] demonstrate that a period of 30–60 min is sufficient for the detection of PARP1-dependent $_b$NAD utilization. After fixation with 4% paraformaldehyde, we detected the biotin label using Avidin-Rhodamine (Sigma), and visualized biotinylated pADPr by confocal microscopy.

Immunohistochemistry. Ovaries dissected in Grace's insect medium were fixed in 4% paraformaldehyde + 0.1% Triton X-100 in PBS for 20 min and blocked with 0.1% Triton X-100 + 1% BSA for 2 h. These ovaries were then incubated with the primary antibody overnight at 4 °C, washed three times with PBS + 0.1% Triton X-100, and incubated with fluorescence-labelled secondary antibody for 2 h at room temperature. After washing three times with PBS + 0.1% Triton X-100, the filamentous actin in the cell membrane was stained with Alexa Fluor 568/633 phalloidin (1:40; Invitrogen) for 30 min, and/or the DNA nuclei were stained with DRAQ5 dye (1:500; Biostatus) for 10 min. The following primary antibodies were used: mouse anti-Orb (4H8, 1:20; DSHB), mouse anti-FasIII (7G10, 1:10; DSHB), mouse anti-Gurken (1D12, 1:10; DSHB), rat anti-DE-cadherin (DCAD2, 1:5; DSHB), rabbit anti-Vasa (1:200; Santa Cruz Biotechnology), mouse anti-hts (1B1,1:20; DSHB), mouse anti-Lamin C (LC28.26, 1:50; DSHB); mouse anti-BAM (1:10; DSHB); rabbit anti-RFP (1:1,000, Clontech). Alexa Fluor 488/568 goat anti-mouse IgG1/Ig2a (1:400; Invitrogen) was used to detect anti-Orb (4H8, IgG1) and anti-FasIII (IgG2a) primary antibodies for double immunostaining. Alexa Fluor 488 goat anti-mouse, Alexa Fluor 568 anti-rabbit and Alexa Fluor 633 anti-rat IgG(H + L) were used to detect other primary antibodies (1:400; Invitrogen). MetaMorph image analysis software (Molecular Devices) was used to quantify the confocal images when required.

RNA–protein ultraviolet-crosslinking analysis. Biotin-labelled RNA probes were made using 0.2 µg PCR templates amplified from DE-cadherin cDNA clone (RE37915; DGRC) with DIG RNA labelling Kit (Roche). A ultraviolet-crosslinking assay was performed following published methods[46,47] with modifications for biotin-labelled probes. The protein lysate from ovaries or the third-instar larvae of the appropriate genotypes was extracted using polysome lysis buffer (100 mM KCl, 5 mM $MgCl_2$, 10 mM HEPES, pH 7.0, 0.5% NP-40, 1 mM DTT). The 50 µg lysate was incubated with 40 pg biotin-labelled RNA probe in a 50 µl volume with 5× binding buffer (50 mM Tris-HCl, 250 mM KCl, 5 mM DTT, pH 7.5) on ice for 15 min. The binding reaction was irradiated with 254 nm ultraviolet light for 10 min on ice using Spectrolinker UV Crosslinker (Krackeler Scientific Inc., Albany, NY). The RNA probes were further digested with 10 µg RNAse A (Sigma) and 1,000 U RNAse T1 (Ambion) for 15 min at 37 °C. For IP, the reaction with 150 µl polysome lysis buffer was incubated with the rabbit anti-Hrp38 antibody[34] or rabbit IgG (Sigma; the negative control) at 1:20 dilution overnight and then with 30 µl protein A agarose (Invitrogen) for 2 h at 4 °C. The IP complex was washed using the lysis buffer three times and resolved in 4–12% PAGE gel (Invitrogen). The protein covalently linked to a stub of the biotin-labelled RNA probe was detected with stabilized streptavidin-horseradish peroxidase conjugate with chemiluminescent substrate (Pierce). The blot was stripped and probed with the rabbit anti-Hrp38 antibody (1:10,000). All crosslinking experiments were repeated three times.

RNA electrophoretic mobility shift assay. RNA electrophoretic mobility shift assay was performed as described earlier[19]. The full-length Hrp38 protein was generated through the cleavage of GST tag by PreScission Protease (GE Healthcare) from GST-Hrp38 recombinant protein, which was expressed from the GST-Hrp38 fusion protein plasmid[34] (a gift from Drs Borah and Steitz). Hrp38 protein was further purified using GSTrap HP columns (GE Healthcare). Either 50 ng GST (BioVision) or 50 ng Hrp38 was incubated with 0.1 µm biotin-labelled G-rich element (413-5′-CAGGGCGCGCACUGUACGAG-3′-432) within the 5′UTR of the *DE-cadherin* gene (IDT) in binding buffer (Pierce). For the pADPr inhibition assay, 50 ng Hrp38 was preincubated with 140 ng pADPr (Biomol) in 1× binding buffer for 20 min at 25 °C. The experiment was repeated three times. The biotin signals from electrophoretic mobility shift assay were detected with a chemiluminescent kit (Pierce) and measured using the Image J software (NIH).

Dual-luciferase reporter assay. A bicistronic luciferase reporter plasmid (pMB255) containing Poliovirus IRES element[48] (a gift from Dr Roegiers) was digested with *Kpn*I and *Eco*RV to remove Poliovirus IRES completely. DE-cadherin 5′ and 3′UTR PCR products were cloned into the derived luciferase reporter in the forward or reverse orientation. The reporter plasmid (pMB255) was also digested with *Eco*RV and *Pml*I and religated as a negative control for firefly luciferase assay. *Drosophila* S2 cells were maintained at 22 °C in the culture medium supplemented with 10% fetal bovine serum and 1% penicillin/streptomycin. A total of 0.5×10^6 cells per well were seeded into a 6-well plate and incubated for 24 h before the transfection. One microgram of plasmid from the different constructs was transfected into S2 cells using Effectene transfection reagent (Qiagen). After the incubation for 24 h, the firefly and Renilla luciferase activities were measured in triplicate using Dual-Luciferase® reporter assay system (Promega). The ratio of the firefly-to-Renilla luciferase activity was calculated based on experiments performed in triplicate, beginning from the transfection. The statistical analysis was done based on Student's *t*-test.

References

1. Fuller, M. T. & Spradling, A. C. Male and female *Drosophila* germline stem cells: two versions of immortality. *Science* **316,** 402–404 (2007).
2. Xie, T. & Spradling, A. C. Decapentaplegic is essential for the maintenance and division of germline stem cells in the *Drosophila* ovary. *Cell* **94,** 251–260 (1998).
3. Wang, Z. & Lin, H. Nanos maintains germline stem cell self-renewal by preventing differentiation. *Science* **303,** 2016–2019 (2004).
4. Szakmary, A., Cox, D. N., Wang, Z. & Lin, H. Regulatory relationship among piwi, pumilio, and bag-of-marbles in *Drosophila* germline stem cell self-renewal and differentiation. *Curr. Biol.* **15,** 171–178 (2005).
5. Maines, J. Z., Park, J. K., Williams, M. & McKearin, D. M. Stonewalling *Drosophila* stem cell differentiation by epigenetic controls. *Development* **134,** 1471–1479 (2007).
6. Song, X., Zhu, C. H., Doan, C. & Xie, T. Germline stem cells anchored by adherens junctions in the *Drosophila* ovary niches. *Science* **296,** 1855–1857 (2002).
7. de Cuevas, M., Lilly, M. A. & Spradling, A. C. Germline cyst formation in *Drosophila*. *Annu. Rev. Genet.* **31,** 405–428 (1997).
8. O'Reilly, A. M., Lee, H. H. & Simon, M. A. Integrins control the positioning and proliferation of follicle stem cells in the *Drosophila* ovary. *J. Cell Biol.* **182,** 801–815 (2008).
9. Godt, D. & Tepass, U. *Drosophila* oocyte localization is mediated by differential cadherin-based adhesion. *Nature* **395,** 387–391 (1998).
10. Gonzalez-Reyes, A. & St Johnston, D. The *Drosophila* AP axis is polarised by the cadherin-mediated positioning of the oocyte. *Development* **125,** 3635–3644 (1998).
11. Dreyfuss, G., Kim, V. N. & Kataoka, N. Messenger-RNA-binding proteins and the messages they carry. *Nat. Rev. Mol. Cell Biol.* **3,** 195–205 (2002).
12. Norvell, A., Kelley, R. L., Wehr, K. & Schüpbach, T. Specific isoforms of Squid, a *Drosophila* hnRNP, perform distinct roles in Gurken localization during oogenesis. *Genes Dev.* **13,** 864–876 (1999).
13. Hachet, O. & Ephrussi, A. *Drosophila* Y14 shuttles to the posterior of the oocyte and is required for oskar mRNA transport. *Curr. Biol.* **11,** 1666–1674 (2001).
14. Cáceres, L. & Nilson, L. A. Translational repression of gurken mRNA in the *Drosophila* oocyte requires the hnRNP Squid in the nurse cells. *Dev. Biol.* **326,** 327–334 (2009).
15. Huynh, J. R., Munro, T. P., Smith-Litiere, K., Lepesant, J. A. & St. Johnston, D. The *Drosophila* hnRNPA/B homolog, Hrp48, is specifically required for a distinct step in osk mRNA localization. *Dev. Cell* **6,** 625–635 (2004).
16. Yano, T. *et al.* Hrp48, a *Drosophila* hnRNPA/B homolog, binds and regulates translation of oskar mRNA. *Dev. Cell* **6,** 637–648 (2004).
17. Jain, R. A. & Gavis, E. R. The *Drosophila* hnRNP M homolog Rumpelstiltskin regulates nanos mRNA localization. *Development* **135,** 973–982 (2008).
18. Tulin, A., Chinenov, Y. & Spradling, A. Regulation of chromatin structure and gene activity by Poly(ADP-ribose) polymerases. *Curr. Top. Dev. Biol.* **56,** 55–83 (2003).
19. Ji, Y. & Tulin, A. V. Poly(ADP-ribosyl)ation of heterogeneous nuclear ribonucleoproteins modulates splicing. *Nucleic Acids Res.* **37,** 3501–3513 (2009).
20. Bonicalzi, M. E., Haince, J. F., Droit, A. & Poirier, G. G. Regulation of poly(ADP-ribose) metabolism by poly(ADP-ribose) glycohydrolase: where and when? *Cell. Mol. Life Sci.* **62,** 739–750 (2005).
21. Tulin, A. & Spradling, A. C. Chromatin loosening by poly(ADP)-ribose polymerase (PARP) at *Drosophila* puff loci. *Science* **299,** 560–562 (2003).
22. Thibault, S. T. *et al.* A complementary transposon tool kit for *Drosophila melanogaster* using P and piggyBac. *Nat. Genet.* **36,** 283–287 (2004).
23. Parks, A. L. *et al.* Systematic generation of high-resolution deletion coverage of the *Drosophila melanogaster* genome. *Nat. Genet.* **36,** 288–292 (2004).
24. Haynes, S. R., Johnson, D., Raychaudhuri, G. & Beyer, A. L. The *Drosophila* Hrb87F gene encodes a new member of the A and B hnRNP protein group. *Nucleic Acids Res.* **19,** 25–31 (1991).
25. McKearin, D. & Ohlstein, B. A role for the *Drosophila* bag-of-marbles protein in the differentiation of cystoblasts from germline stem cells. *Development* **121,** 2937–2947 (1995).
26. Chen, D. & McKearin, D. Dpp signaling silences bam transcription directly to establish asymmetric divisions of germline stem cells. *Curr. Biol.* **13,** 1786–1791 (2003).
27. Li, Y., Minor, N. T., Park, J. K., McKearin, D. M. & Maines, J. Z. Bam and Bgcn antagonize Nanos-dependent germ-line stem cell maintenance. *Proc. Natl Acad. Sci. USA* **106,** 9304–9309 (2009).
28. Eliazer, S., Shalaby, N. A. & Buszczak, M. Loss of lysine-specific demethylase 1 nonautonomously causes stem cell tumors in the *Drosophila* ovary. *Proc. Natl Acad. Sci. USA* **108,** 7064–7069 (2011).
29. Haynes, S. R., Raychaudhuri, G. & Beyer, A. L. The *Drosophila* Hrb98DE locus encodes four protein isoforms homologous to the A1 protein of mammalian heterogeneous nuclear ribonucleoprotein complexes. *Mol. Cell. Biol.* **10,** 316–323 (1990).
30. Burd, C. G. & Dreyfuss, G. RNA binding specificity of hnRNP A1: significance of hnRNP A1 high-affinity binding sites in pre-mRNA splicing. *EMBO J.* **13,** 1197–1204 (1994).
31. Misra, S. *et al.* Annotation of the *Drosophila melanogaster* euchromatic genome: a systematic review. *Genome Biol.* **3,** RESEARCH0083 (2002).
32. Gilbert, W. V. Alternative ways to think about cellular internal ribosome entry. *J. Biol. Chem.* **285,** 29033–29038 (2010).
33. Villa-Cuesta, E., Sage, B. T. & Tatar, M. A role for *Drosophila* dFoxO and dFoxO 5UTR internal ribosomal entry sites during fasting. *PLoS ONE* **5,** e11521 (2010).
34. Borah, S., Wong, A. C. & Steitz, J. A. *Drosophila* hnRNP A1 homologs Hrp36/Hrp38 enhance U2-type versus U12-type splicing to regulate alternative splicing of the prospero twintron. *Proc. Natl Acad. Sci. USA* **106,** 2577–2582 (2009).
35. Bonnal, S. *et al.* Heterogeneous nuclear ribonucleoprotein a1 is a novel internal ribosome entry site trans-acting factor that modulates alternative initiation of translation of the fibroblast growth factor 2 mRNA. *J. Biol. Chem.* **280,** 4144–4153 (2005).
36. Jo, O. D. *et al.* Heterogeneous nuclear ribonucleoprotein A1 regulates cyclin D1 and c-myc internal ribosome entry site function through Akt signaling. *J. Biol. Chem.* **283,** 23274–23287 (2008).
37. Shi, Y. *et al.* IL-6-induced stimulation of c-Myc translation in multiple myeloma cells is mediated by Myc internal ribosome entry site function and the RNA-binding protein, hnRNP A1. *Cancer Res.* **68,** 10215–10222 (2008).
38. Lewis, S. M. & Holcik, M. For IRES trans-acting factors, it is all about location. *Oncogene* **27,** 1033–1035 (2007).
39. Leung, A. K. *et al.* Poly(ADP-Ribose) regulates stress responses and microRNA activity in the cytoplasm. *Mol. Cell* **42,** 489–499 (2011).
40. Oda, H., Uemura, T. & Takeichi, M. Phenotypic analysis of null mutants of *DE*-cadherin and Armadillo in *Drosophila* ovaries reveals distinct aspects of their functions in cell adhesion and cytoskeletal organization. *Genes Cells* **2,** 29–40 (1997).
41. Fichelson, P., Jagut, M., Lepanse, S., Lepesant, J. A. & Huynh, J. R. Lethal giant larvae is required with the par genes for the early polarization of the *Drosophila* oocyte. *Development* **137,** 815–824 (2010).
42. Hanai, S. *et al.* Loss of poly(ADP-ribose) glycohydrolase causes progressive neurodegeneration in *Drosophila* melanogaster. *Proc. Natl Acad. Sci. USA* **101,** 82–86 (2004).
43. Chou, T. B. & Perrimon, N. Use of a yeast site-specific recombinase to produce female germline chimeras in *Drosophila*. *Genetics* **131,** 643–653 (1992).
44. Duffy, J., Harrison, D. & Perrimon, N. Identifying loci required for follicular patterning using directed mosaics. *Development* **125,** 2263–2271 (1998).
45. Bakondi, E. *et al.* Detection of poly(ADP-ribose) polymerase activation in oxidatively stressed cells and tissues using biotinylated NAD substrate. *J. Histochem. Cytochem.* **50,** 91–98 (2002).
46. Walker, J., de Melo Neto, O. & Standart, N. Gel retardation and UV-crosslinking assays to detect specific RNA-protein interactions in the 5′or 3′

UTRs of translationally regulated mRNAs. *Methods Mol. Biol.* **77,** 365–378 (1998).
47. Goodrich, J. S., Clouse, K. N. & Schüpbach, T. Hrb27C, Sqd and Otu cooperatively regulate gurken RNA localization and mediate nurse cell chromosome dispersion in *Drosophila* oogenesis. *Development* **131,** 1949–1958 (2004).
48. Bolinger, C. *et al.* RNA helicase A interacts with divergent lymphotropic retroviruses and promotes translation of human T-cell leukemia virus type 1. *Nucleic Acids Res.* **35,** 2629–2642 (2007).

Acknowledgements

We thank Drs S. Borah, A. O'Reilly, F. Roegiers, H. Saumweber, J.A. Steitz and M. Takeichi for providing materials. Drs A. O'Reilly, E. Pechenkina and D. Martin contributed valuable comments on the manuscript. This project is funded by the National Institutes of Health (R01 GM077452) to A.V.T.

Author contributions

Y.J. and A.V.T. designed research; performed research; contributed new reagents/analytic tools; analysed data; and wrote the paper.

Additional information

Supplementary Information accompanies this paper at http://www.nature.com/naturecommunications

Competing financial interests: The authors declare no competing financial interests.

Reprints and permission information is available online at http://npg.nature.com/reprintsandpermissions/

How to cite this article: Ji, Y. *et al.* Poly(ADP-ribose) controls DE-cadherin-dependent stem cell maintenance and oocyte localization. *Nat. Commun.* 3:760 doi: 10.1038/ncomms1759 (2012).